Simulation of Ca^{2+} and Mg^{2+} Solvation Using Polarizable Atomic Multipole Potential

Dian Jiao,[†] Christopher King,[†] Alan Grossfield,[‡] Thomas A. Darden,[§] and Pengyu Ren*,[†]

Department of Biomedical Engineering, The University of Texas Austin, Austin, Texas 78712, IBM Thomas J. Watson Research Center, Yorktown Heights, New York 10598, and National Institute of Environmental Health Sciences, Research Triangle Park, North Carolina 27709

The alkaline earth metals calcium and magnesium are critically involved in many biomolecular processes. To understand the hydration thermodynamics of these ions, we have performed molecular dynamics simulations using a polarizable potential. Particle-mesh Ewald for point multipoles has been applied to the calculation of electrostatic interactions. The parameters in this model have been determined from an ab initio quantum mechanical calculation of dimer interactions between ions and water. Two methods for ion solvation free energy calculation, free energy perturbation, and the Bennett acceptance ratio have been compared. Both predict results consistent with other theoretical estimations while the Bennett approach leads to a much smaller statistical error. Based on the Born theory and the ion−oxygen radial distribution functions, we estimate the effective size of the ions in solution, concluding that K$^+$ > Na$^+$ ≅ Ca^{2+} > Mg^{2+}. There appears to be much stronger perturbation in water structure, dynamics, and dipole moment around the divalent cations than the monovalent K$^+$ and Na$^+$. The average water coordination numbers for Ca^{2+} and Mg^{2+} are 7.3 and 6, respectively. The lifetime of water molecules in the first solvation shell of Mg^{2+} is on the order of hundreds of picoseconds, in contrast to only few picoseconds for Ca^{2+}, K$^+$, or Na$^+$.

I. Introduction

Ions play critical roles in fundamental biological functions including signal transduction, enzymatic activities, and organizing the structure of proteins and nucleic acids. Besides acting as nonspecific salt buffers, ions also interact with biomolecules in specific fashions (e.g., ion channels, metalloproteases). In fact, many biological processes have been found to be ion specific. For example, Mg^{2+} is critical to stabilize the three-dimensional structure of many functional RNA molecules; protein kinases require Mg^{2+} in coordination with ATP to facilitate phosphorylation; the binding of Ca^{2+} to calmodulin is involved in DNA synthesis and cell division.[1] In addition, a recent review has underscored the importance of Zn^{2+} and other metal ions in survival and pathogenesis of many viruses, including HIV, hepatitis, herpes simplex, Rubella, and influenza virus.[2] Even though both are divalent ions of slightly different sizes, the abilities of calcium and magnesium ions to coordinate with ligands differ. Experimentally, it has been shown that Mg^{2+} binds six water molecules in an octahedral organization,[3] while the coordination number of Ca^{2+}, reported from various X-ray, neutron diffraction and EXAFS experiments, varies from 6 to 10.[4−7]

Ion solvation thermodynamics has been of great interest, as the interplay between the ion−water and ion−protein interactions may provide the basis for ion selection. Ab initio molecular dynamic simulations of ion solvation have been reported.[8−10] However, most of the ab initio studies are limited to small systems of a few water molecules for a few picoseconds. Hybrid QM/MM approaches have also been attempted in the investiga-

tion of ion solvation properties.[11−15] The quasi-chemical approach treats interactions between ions and immediate water molecules (inner-shell) quantum mechanically, while applying less expensive dielectric continuum techniques to model the bulk solvent.[16,17] This approach has produced solvation thermodynamics consistent with experimental data for a wide variety of ions.[18,19] However, applying even moderate-level quantum mechanics methods to larger systems such as proteins in solution is prohibitively expensive. This explains the appeal of classical molecular dynamics simulations. Because extensive simulations are possible, one can derive detailed atomic level information pertaining to thermodynamics, structure, and kinetics. However, classical models are only as good as the potential functions and parameters used; in the case of simple ions, this means that quantitative ion solvation thermodynamic data, such as ion solvation free energies, is required a priori in order to arrive at sensible parameters. Unfortunately, single ion solvation free energies cannot be measured experimentally; only the relative solvation free energies of like-charged ions or the totally solvation free energies for a neutral salt are directly accessible. A number of techniques exist which purport to separate the cation and anion contributions, but each involves an unverifiable extrathermodynamic assumption, with the result that published single ion solvation values vary wildly.[20] Polarizable force fields avoid the ambiguity of parametrizing against these values; because they account for many-body effects, their parameters can be determined in the gas phase, where extra assumptions are unnecessary, and extended to solution with confidence.[20−23]

Previously, a polarizable molecular mechanic model was successfully applied to the study of solvation of monovalent ion in water and other solvents.[20,24] In this model, electrostatics is represented by atomic multipole moments with explicit atomic dipole induction.[25,26] The Thole dipole induction model adopted by our model has been compared favorably with other ap-

* Corresponding author phone: 512 232 1832; fax: 512 471 0616; e-mail: pren@mail.utexas.edu.
† The University of Texas Austin.
‡ IBM Thomas J. Watson Research Center.
§ National Institute of Environmental Health Sciences.

proaches to describe polarization effects.[27] In this study, we report the extension of this polarizable model to divalent calcium and magnesium ions' interactions with water. Divalent ions present particular challenges for classical simulations due to the high charge density and strong polarization effect. Ab initio calculations of ion−water interaction in gas-phase are utilized to derive the ion van der Waals parameters. Molecular dynamics simulation of ion solvation using Particle-mesh Ewald is described. Ion solvation free energies are computed from both free-energy perturbation (FEP) and Bennett acceptance ratio (BAR) methods. Ion solvation structures and dynamics from the molecular dynamics simulations are compared with those of monovalent ions as well as experimental and other theoretical results.

II. Methods

A. Potential Energy Model. The potential model used in this work is based on the one previously reported for water, K^+, Na^+, and Cl^-.[20,26] Therefore, we will briefly summarize the aspects that are more relevant to this work. The electrostatic component of the force field is described by a set of permanent atomic multipoles. In this work, only point charges are placed on the ions, and the higher order moments are used for the water molecules. The polarization effect is accounted for via atomic dipole induction:

$$\mu_{i,\alpha}^{ind} = \alpha_i \left(\sum_{\{j\}} T_\alpha^{ij} M_j + \sum_{\{j'\}} T_{\alpha\beta}^{ij'} \mu_{j',\beta}^{ind} \right) \quad \text{for } \alpha,\beta = 1,2,3 \quad (1)$$

where $M_j = [q_j, \mu_{j,1}, \mu_{j,2}, \mu_{j,3},...]^T$ represents the permanent charge, dipole and quadrupole moments. $T_\alpha^{ij} = [T_\alpha, T_{\alpha 1}, T_{\alpha 2}, T_{\alpha 3},...]$ is the interaction matrix between two atoms i and j. The Einstein convention implying a summation over repeated subscripts is used. α_i is the atomic polarizability of ion and water. The first term in the parentheses corresponds to the induction field due to the permanent multipoles while the second is due to induced dipoles produced at the other atoms. A transferable isotropic polarizability for each chemical element was derived by fitting to experimental polarizabilities of a set of molecules. The atomic polarizabilities for divalent caions are generally small and were derived from ab initio calculations in this study.

The polarization energy, field and force are damped at short distance (<5 Å) according to Thole's scheme[28] to avoid polarization catastrophe, where the induced dipoles of two interacting sites approach infinity upon mutual induction. Such a "catastrophe" occurs as a result of the point approximation used in the polarizability model. Thole proposed to "damp" the dipole interaction at short range by replacing the point charge in a pairwise interaction by a smeared charge distribution of the following form:

$$\rho = \frac{3a}{4\pi} \exp(-au^3) \quad (2)$$

where $u = R_{ij}/(\alpha_i\alpha_j)^{1/6}$ is the effective distance between atom i and j. The scalar a is a dimensionless parameter corresponding to the width of the smeared charge distribution that effectively controls the damping strength. A lower value leads to stronger damping and less polarization energy. Based on water cluster association energy, a value of 0.39 has been derived previously. A recent ab initio study of ion−water interaction has demonstrated that stronger damping for metal ions gives a better induced dipole moment on the water molecule.[29] We have

chosen to adjust the damping coefficients for polariation between the divalent ion and water molecules.

The repulsion−dispersion or van der Waals interaction between atoms is described using a buffered 14−7 function.

$$U_{ij}^{buff} = \epsilon_{ij} \left(\frac{1+\delta}{\rho_{ij}+\delta} \right)^{n-m} \left(\frac{1+\gamma}{\rho_{ij}^m+\gamma} - 2 \right) \quad (3)$$

where ϵ_{ij} is the potential well depth. ρ_{ij} equals R_{ij}/R_{ij}^0 with R_{ij} as the separation distance between atoms i and j, and R_{ij}^0 the minimum energy distance. Following Halgren,[30] we used fixed values of $n = 14$, $m = 7$, $\delta = 0.07$, and $\gamma = 0.12$. Thus, the only free parameters for Ca^{2+} and Mg^{2+} are R and ϵ.

B. Ab initio Calculations and Parametrization. Ab initio calculations were performed using the Gaussian 03 package.[31] The atomic polarizabilities of both ions are determined from B3LYP/6-31G* calculation. The geometry of ion−water dimer was fully optimized using this level of theory, followed by single point energy calculations at these geometries using MP2 calculations. Ion−oxygen separation distance was varied between 1.5 and 5 Å with water geometry fixed at the optimized orientation, and the binding energy was subsequently obtained for each distance. The binding energies were computed as the total energy minus the isolated water and ion energies at infinite separation distance. Basis-set superimposition error (BSSE) was removed in all calculations. Both MP2/6-311++G(3df,3pd) and MP2/aug-cc-pVTZ basis sets were used for Mg^{2+}, and MP2/6-311++G(3df,3pd) for Ca^{2+}. The distance dependence of dimer binding energies was used to adjust vdW parameters (R and ϵ) and damping factors (a) of Ca^{2+} and Mg^{2+}.

C. Free Energy Simulations. The ion solvation free energies of Ca^{2+} and Mg^{2+} were computed from molecular dynamics simulations. First, we computed the solvation free-energy for a neutral vdW particle by running 12 independent simulations, which varied the calcium vdW parameters according to

$$R(\lambda) = 1 + \lambda(R_{final} - 1) \quad (4)$$

$$\epsilon(\lambda) = \lambda(\epsilon_{final}) \quad (5)$$

for $\lambda = (0.01, 0.1, 0.2, 0.3, 0.4, 0.5, 0.6, 0.7, 0.8, 0.9, 1.0)$. This was followed by 12 simulations during which the ion's charge and polarizability were set to

$$q(\lambda) = \lambda(q_{final}) \quad (6)$$

$$\alpha(\lambda) = \lambda(\alpha_{final}) \quad (7)$$

for $\lambda = (0.01, 0.05, 0.1, 0.2, 0.3, 0.4, 0.5, 0.6, 0.7, 0.8, 0.9, 1.0)$. The Ca^{2+} ion was then perturbed to Mg^{2+} by changing both the vdW parameters and damping coefficient in three steps.

Molecular dynamics simulations were performed using the TINKER package.[32] The long-range electrostatics is treated using particle-mesh Ewald summation for atomic multipoles[33] with a cutoff of 7 Å in the real space and 0.75 Å spacing and fifth-order spline in the reciprocal space. Induced dipoles were iterated until the changes in atomic induced dipoles were less than 0.01 D. Molecular dynamics simulations were performed with a 1 fs time step for 300 ps. Coordinates of all atoms were saved every 0.1 ps, with the first 50 ps discarded as equilibration. The temperature was maintained at 298 K using the Berendsen weak coupling method.[34] To investigate the effect of system size, a single ion was placed in a periodic cubic box of either 216 or 512 water molecules, with 18.64 or 25 Å on a side.

The Helmholtz free-energy changes between adjacent simulations were calculated two different ways, first using free-energy perturbation (FEP) methods,[35] then by using the Bennett acceptance ratio (BAR) method.[36] In the standard FEP approach, the free-energy changes between adjacent steps were computed as the average of the forward and backward perturbations, and the error for each step was estimated from the difference between the average and the forward or backward perturbation result. The overall error was computed as the sum of errors of all constituent steps. Using the Bennett formation, the free energy change between simulations λ_i and λ_{i+1} was computed iteratively using

$$\Delta A(j)_{\lambda_i \to \lambda_{i+1}} = \ln\frac{\langle 1/[1 + \exp((E_{\lambda_i} - E_{\lambda_{i+1}} + C)/RT)]\rangle_{\lambda_{i+1}}}{\langle 1/[1 + \exp((E_{\lambda_{i+1}} - E_{\lambda_i} - C)/RT)]\rangle_{\lambda_i}} + C - \ln\frac{n_{\lambda_{i+1}}}{n_{\lambda_i}} \quad (8)$$

where C is given by

$$C = \Delta A(j - 1) \quad (9)$$

and j is the current iteration. Here, $E_{\lambda i}$ is the total energy of the system evaluated using the parameters from λ_i. The subscripts outside the averaging brackets denote the MD trajectory used for evaluation of E. The variable n is the number of trajectory snapshots in each simulation. For $j = 1$, the initial value of $C = \Delta A(0)$ was given an arbitrary value as a rough estimate of the free energy change. Iterations continued until the value of $(C - \Delta A) < 0.01$ kcal/mol. The final values calculated for ΔA were independent of the initial values given for C. The statistical error of BAR method was estimated as the sum of the square root of the variance of ΔA between successive simulations according to the following:

$$\sigma^2_{\lambda_i \to \lambda_{i+1}} = \frac{\langle f^2 \rangle_{\lambda_i} - \langle f \rangle^2_{\lambda_i}}{n\lambda_i \langle f \rangle^2_{\lambda_i}} + \frac{\langle f^2 \rangle_{\lambda_{i+1}} - \langle f \rangle^2_{\lambda_{i+1}}}{n\lambda_i \langle f \rangle^2_{\lambda_i}} \quad (10)$$

$$\langle f \rangle_{\lambda_i} = \langle 1/1 + \exp((E\lambda_{i+1} - E\lambda_i - C)/RT) \rangle \lambda_i$$

$$\langle f \rangle_{\lambda_{i+1}} = \langle 1/1 + \exp((E\lambda_i - E\lambda_{i+1} + C)/RT) \rangle \lambda_{i+1} \quad (11)$$

where C is the final free energy value calculated from BAR method. In the above formula, n refers to the number of random samples that are independent of each other. In our calculations, we estimated the error during the particle growth by counting every 0.5 ps as one independent data point, and every 1 ps during charging based on the relaxation time scale of bulk water and water molecules in the first solvation shell. The error for the free-energy change from Ca²⁺ to Mg²⁺ could be underestimated as the water molecules around Mg²⁺ relax at a much slower scale as will be discussed below.

The structure and dynamics of water molecules in the first solvation shell are analyzed using the MD trajectory from the final charging stage, where the ion is fully charged. All results are based on the simulation of the 512 water system. In the remaining analysis, we define the ion's first solvation shell to be all water molecules positioned within the first minimum of the radial distribution function (RDF) of the O-ion. For Mg²⁺, additional 300 ps simulations (total 600 ps) have been performed to investigate the dynamics. Time correlation functions have been computed for the fluctuation of the first shell coordination
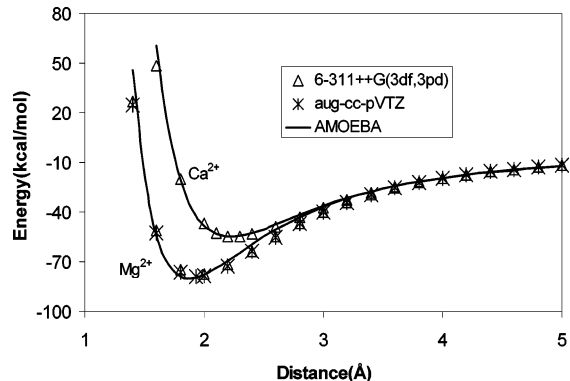

Figure 1. Ion−water dimer binding energy in gas phase as a function of ion and oxygen separation distance.

TABLE 1: Parameters for Ions[a]

ion	R	ε	α	α
Ca²⁺	3.63	0.35	0.55	0.159
Mg²⁺	3.21	0.28	0.08	0.095

[a] R and ϵ are diameter and well depth for van der Waals potential in Å and kcal/mol, respectively. α is the polarizability in Å³. a is the dimensionless damping coefficient in eq 2.

number, from which the relaxation time of the first shell water is derived using an exponential decay model.[24]

III. Results and Discussion

A. Gas-Phase Ion−Water Dimer Interaction. A polarizable potential is capable of capturing the many-body effect in electrostatics when moving from one environment to another. As a result, parameters in the polarizable models can be conveniently determined and verified by comparison to high-level ab initio results in the gas-phase, as was previously demonstrated for monovalent ions.[20] With the water model from previous work,[26] and the polarizabilities of Ca²⁺ and Mg²⁺ derived from DFT, the parameters remaining to be determined were primarily the van der Waals R and ϵ for each ion. We have chosen the vdW parameters to best match the ab initio binding energies of the ion−water dimer in the gas-phase. The same approach has been shown to be effective in our previous study of K⁺ and Na⁺. An additional parameter, the damping coefficient, has been adjusted for the divalent ions to modify the polarization between the cation and other atoms at short distances. A recent investigation on dipole induction between the cation and water molecules has shown that Thole's induction model overestimates the induced dipole moments at short range when the original damping coefficient is used.[29] As this was not the case for a point charge polarizing a water molecule, this effective reduction in polarizability has been attributed to the repulsion between the electron distributions of the ion and water. We indeed found it necessary to reduce the damping coefficient (enhance the damping) in order to match the ab initio equilibrium dimer binding energy and separation simultaneously. When our standard damping coefficient, 0.39, is used, the equilibrium dimer separation distance is shorter than the ab initio distance by 5% when the binding energies agree. Figure 1 compares the distance dependence of binding energies given by the final model and ab initio calculations. The final parameters of the two cations are listed in Table 1. The two basis sets used for Mg²⁺ in ab initio calculations gave consistent binding energies over a range of distances. The agreement between the final model and ab initio results is rather satisfactory. As expected, Mg²⁺ binds stronger than Ca²⁺ to water. The

TABLE 2: Solvation Free Energy of Calcium and Magnesium Ion in Water[a]

		216 water	512 water	Schmid et al.[b]	Asthagiri et al.[c]
Ca^{2+}	FEP	−359.5 (7.0)	−360.3 (13.8)	−357.2	−354.7
	BAR	−357.4 (2.0)	−354.9 (1.7)		
Mg^{2+}	BAR		−431.1 (2.9)	−435.4	−433.3

[a] The number in parentheses is the estimated error. 1 M in gas phase is chosen as the standard state. [b] Ref 38. [c] Ref 18.

equilibrium distance between Mg^{2+} and water is 0.3 Å shorter than that of Ca^{2+}-water while the equilibrium binding energy is lower by 25 kcal/mol.

B. Solvation Thermodynamics. The solvation free energy is the key quantity describing the thermodynamic stability of an ion in solution. Solvation free energies of calcium and magnesium ions in water have been computed from molecular dynamics simulations where a single ion is grown gradually in a water box by first turning on its vdW parameters, then the ionic charges and polarizabilities. Table 2 lists the solvation free energies of Ca^{2+} and Mg^{2+}, which are about 4−5 times greater than those of monovalent K^+ and Na^+ reported previously.[20] For the purpose of comparison, two different approaches, FEP and BAR, were used to obtain solvation free energies of Ca^{2+} based on the same set of simulations. The results show that using the BAR method significantly reduces the statistical uncertainty using the same amount of simulation data, in agreement with what others have observed.[37] Further, for the system under study, the difference between the free energies computed by FEP and BAR occurs mostly for charge growth beyond 1 e, where the effective energy change between successive stages is largest. The solvation free energy of Mg^{2+} is obtained by turning a Ca^{2+} ion into a Mg^{2+} ion through adjustment of the vdW and damping parameters. Increasing the system size from 216 to 512 waters leads to small changes in the solvation free energy within the statistical uncertainty. The free energies from the BAR method compare favorably to those from quasi-chemical method[18] and the theoretical evaluation of Schmid.[38] In the quasi-chemical method, the ion and immediately adjacent water molecules are treated quantum mechanically and kept fixed while the surrounding water is described by classical mechanics. Recently, the same group has confirmed the there is indeed an "inner" shell of four water molecules around K^+ using ab initio molecular dynamics.[19] Due to the fact that, experimentally, it is only possible to measure the solvation free energy of whole salts, extrathermodynamic assumptions are used in order to determine the contributions from the cations and anions. By setting the proton hydration free energy, Schmid was able to estimate solvation free energies of other ions based on experimental free energies of whole salt.

The classic Born theory of ion solvation states that there exists an effective solvation radius, a_B, for each ion such that the solvation free energy of the ion in a dielectric medium is given by

$$\Delta A = -\frac{q^2}{2a_B}\left(1 - \frac{1}{\epsilon_d}\right) \qquad (12)$$

Where q is the charge of the ion and ϵ_d is the dielectric constant of the medium. We have calculated the effective radius of Na^+, K^+, Ca^{2+}, and Mg^{2+} based on the Born equation and the solvation free energy obtained from our simulations. As shown in Table 3, Mg^{2+} has the smallest radius while K^+ is the largest. Ca^{2+} and Na^+ are almost the same size according to the Born radius. In agreement with the Born equation, the hydration free-

TABLE 3: The Effective Sizes of Ions as Indicated by Born Theory and RDF

	effective Born radius	first peak in ion−O RDF	first minimum in ion−O RDF
Mg^{2+}	1.56	2.07	2.95
Ca^{2+}	1.89	2.41	3.23
Na^{+a}	1.87	2.39	3.29
$K^{+\ a}$	2.30	2.76	3.53

[a] The Born radii for Na+ and K+ are computed based on solvation free energies from ref 20. The RDF values are taken from ref 24.
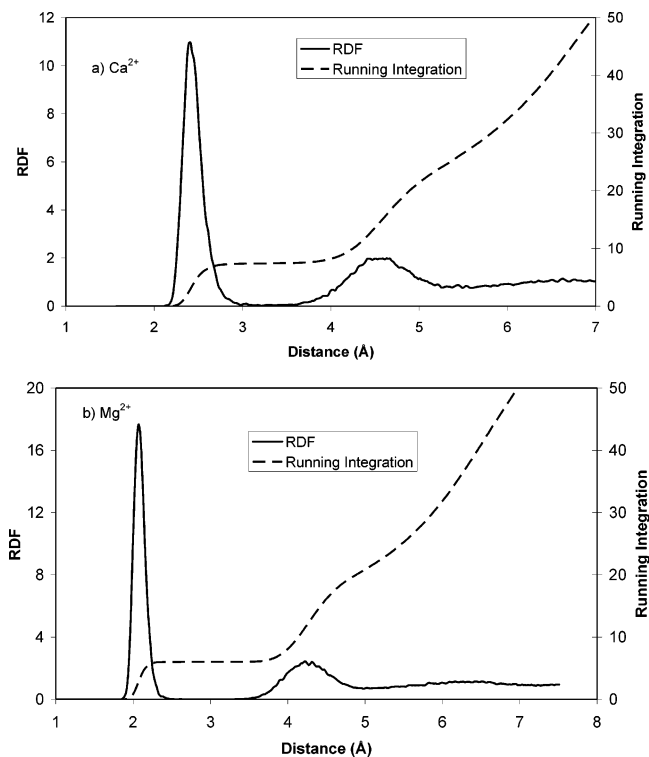
Figure 2. Radial distribution functions of ion and oxygen atom in water. (a) Ca^{2+}, (b) Mg^{2+}

energy calculated during our charge growth simulations of Ca^{2+} indeed displays a quadratic dependence on the magnitude of the charge on the ion. However, it should be noted that previous work has shown that hydration around positively and negatively charged ions is rather different in contrast to the symmetric charge dependence implied by the Born theory.[24,39,40]

C. Solvent Structure and Dynamics. To characterize the structure of water molecules around the ion, the radial distribution function (RDF) has been sampled from the dynamics trajectories. In Figure 2a and 2b, the RDF and their running integrations are shown for Ca−O and Mg−O, respectively. The first peak of the RDF is located at 2.41 Å for Ca^{2+}, 2.07 Å for Mg^{2+}. Previous work reported a first peak at 2.76 Å for K^+, 2.39 Å for Na^+.[24] The order of the first peak location among these ions is consistent with the effective Born radius, i.e., $K^+ > Na^+ \cong Ca^{2+} > Mg^{2+}$. As shown in Table 3, the differences between the effective radii and the first peak positions are almost a constant of 0.5 Å for all four ions. The size of the ion plus the first shell of water molecules is related to the position of the first minimum in RDF. There also appears to be a constant offset of 1.3 Å between an ion's Born radius and the location of the first minimum, which can be considered as the "effective" size of the ion plus first shell water solvent. The heights of the first peaks are much more prominent for Ca^{2+} and Mg^{2+} than for Na^+ and K^+,[24] correlating with the solvation free-energies rather than the size of the ion. The sharp peaks indicate the
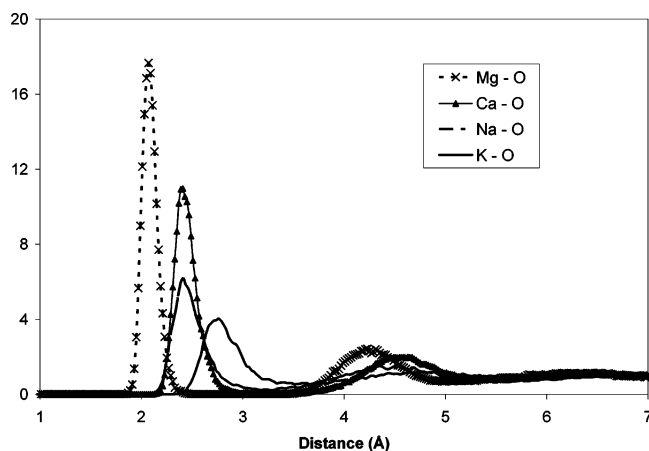
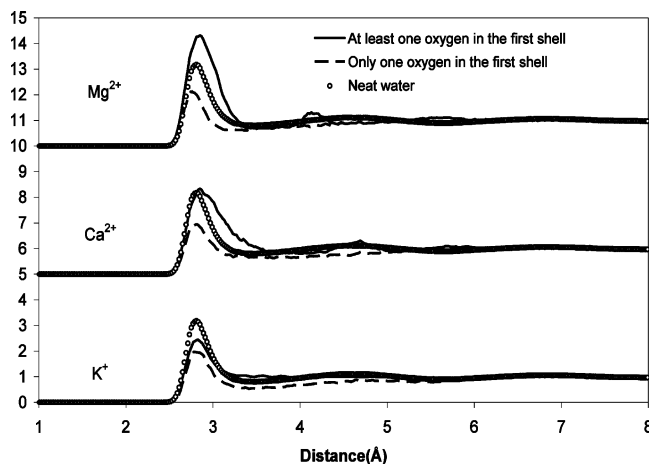**Figure 3.** Comparison of RDFs of mono and divalent cations in water.

Figure 4. Oxygen−oxygen radial distribution functions of water molecules in the first solvation shell. The results for K⁺ are taken from ref 24. RDFs for Ca²⁺ and Mg²⁺ are offset by 10 and 5, respectively.

highly ordered water structure around the divalent ions. Also, the first valleys of Mg−O and Ca−O RDF are wide and flat, in contrast to those of Na⁺ and K⁺, signifying a clear separation between the first and second solvation shells. From the running integration of the RDF, the average coordination number for Mg²⁺ is found to be 6, in agreement with experimental[3] and ab initio MD results.[10] For Ca²⁺, a coordination number of 7.3 was obtained, consistent with an X-ray experimental value of 7.2±1.2. Recent ab initio MD simulations of Ca²⁺ in 60 water molecules reported a value of 6.2 or 7.0 depending on the flexibility of the water molecules used.[9] Thus, our model accurately describes the difference between Ca²⁺ and Mg²⁺ in water coordination.

To examine the effect of the ions on nearby solvent structure, the radial distribution functions of oxygen−oxygen pair in the first solvation shell have been calculated. First, we have computed RDF for oxygen pairs where at least one oxygen atom is in the first solvation shell. Comparison is made between the divalent ions and K⁺ in Figure 4. Interestingly, the O−O RDFs around both Mg²⁺ and Ca²⁺ have more pronounced first peaks than K⁺. In the case of Mg²⁺, the first peak is even higher than the bulk water. The RDFs of Ca²⁺ and Mg²⁺ also display second peaks that do not exist for K⁺. It is, however, possible that these peaks originate from oxygen pairs in the first solvation shell. We have, therefore, also computed RDFs between oxygen pairs with only one oxygen atom in the first shell. As shown in Figure 4, the resulting RDFs have significantly reduced first peak, and the second peaks completely disappear. This dramatic change
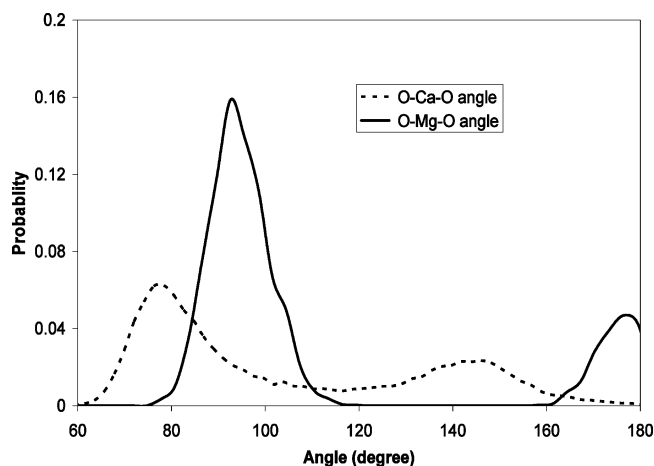

Figure 5. The O−ion−O angle distribution in the first solvation shell.

confirms that the water molecules in the first solvation shell are highly organized by the divalent ions. In contrast, the O−O RDFs of K⁺ display less features than bulk water no matter whether the pairs in the solvation shell are counted or not. The reduced correlation between the water in the first shell and surrounding water signifies the disruption of solvent structure by the cations.

To further describe the organization of water molecules immediately adjacent to the cations, the angle distributions of O−X−O, X = Ca²⁺ or Mg²⁺, sampled from the MD simulations are plotted in Figure 5. The O−Mg−O angle is predominantly distributed around 92° and 176°, indicating an octahedral coordination as also determined by X-ray experiment.[3] In contrast, the O−Ca−O has a much broader distribution that peaks at 78° and 147°.

The ion solvation free-energy is a thermodynamic indicator of how well an ion is solvated in the water, whereas the relative solvation free-energies among different solvents determine the partitioning of the ion between these solvents. However, one must also consider ionic kinetics, which is of great importance whenever the ion changes environments, such as when it enters a channel or binds to a protein. We have investigated the lifetime of ion−water coordination by examining the time correlation function of the instantaneous first shell coordination number. For Ca²⁺, the relaxation time in the first solvation shell is 18 ps and the coordination number fluctuates between 5 and 9 on a time scale of 1 ∼ 2 ps. For Mg²⁺, a relaxation time of 228 ps was obtained, and the coordination number only deviates from 6 briefly during the whole 600 ps simulation. Relaxation times of 0.8 and 1.8 ps were reported previously for K⁺ and Na⁺.[24] These results suggest that the water molecules in the first solvation shell of Mg²⁺ will remain bound for hundreds of picoseconds while the water molecules around Ca²⁺ and monovalent K⁺ and Na⁺ move in and out of the first shell much more frequently.

The self-diffusion coefficients were computed from the mean-squared displacement sampled during MD simulations. The Ca²⁺ exhibits a diffusion coefficient of 0.8×10^{-5} cm² s⁻¹, higher than that of Mg²⁺, 0.3×10^{-5} cm² s⁻¹. The experimentally measured diffusion coefficients for Ca²⁺ and Mg²⁺ are 0.79 and 0.71×10^{-5} cm² s⁻¹, respectively.[41] Spangberg and Hermansson also reported a somewhat lower diffusion constant (0.4×10^{-5} cm² s⁻¹) for Mg²⁺ in water from MD simulations using polarizable potentials. Lower Ca²⁺ and Mg²⁺ diffusion constants have been predicted by molecular dynamics simulations using non polarizable potentials as well.[42,43] The reduction of mobility from Ca²⁺ to Mg²⁺ in our simulation is most likely
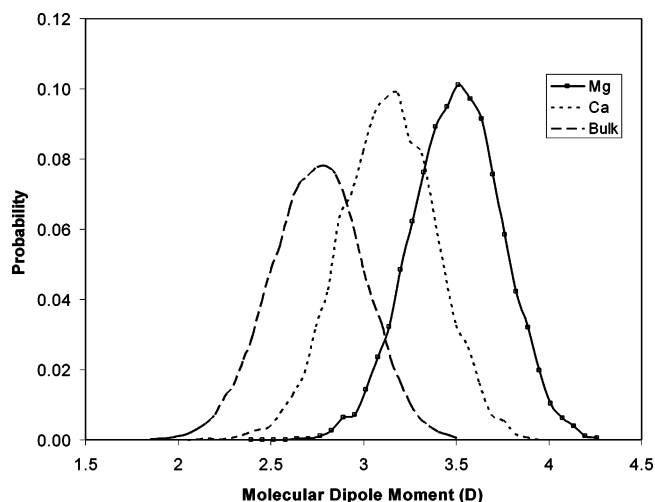
Figure 6. The dipole moment of water molecules in the first solvation shell.

due to the stronger interaction between the latter and water; effectively, we are measuring the diffusion coefficient of a super-particle containing six waters and an ion.

The dipole moment distribution of the water molecule in the first solvation shell is shown in Figure 6. The average dipole moments of water molecules around the ion are greater that that of bulk water (2.77 D) due to the polarization effect. Mg^{2+} displays stronger induction on water than Ca^{2+} likely because of its smaller effective radius as discussed earlier. For Na^+ and K^+, the average molecular dipole moments in the first shell were reported to be roughly the same magnitude as those in bulk.[24] These results suggest that the dipole moment of solvent is affected by both the size and, more importantly, the valence of the ion species. Explicit polarization allows a water's dipole moment to reflect the surrounding electric field, as opposed to a fixed charge model where the dipole is determined solely by the molecule's orientation. While a nonpolarizable potential might be able to describe the solvation around monovalent cations qualitatively, polarizable description is essential for higher valence ions.

Conclusion

A polarizable model has been applied to the simulation of solvation of Mg^{2+} and Ca^{2+} ions in water. The parameters for the ions have been derived based on the ab initio ion−water dimer interaction energies in the gas-phase. The single ion solvation free-energies predicted by molecular dynamics simulations agree well with other theoretical estimations. The resulting solvation free-energies of Ca^{2+} and Mg^{2+} are 4−5 times greater than those of K^+ and Na^+. The Bennett acceptance ratio method appears to be more accurate and computationally more efficient than the traditional free-energy perturbation approach for free-energy calculations. The use of a 216- or 512-water system leads to slightly different (∼ 1%) solvation free-energies for Ca^{2+}.

The results of molecular dynamics simulations suggest that the divalent cations perturb the structure and dipole moments of the first solvation shell water considerably, in contrast to monovalent cations. The water structures in the first solvation shells of the divalent caions are more structured that those around monovalent cations, demonstrated by the sharp first peak in the RDFs. Additionally, the separation between the first and second shell is more prominent. Based on the RDF and Born theory, the effective sizes of the ions compared in this study are in the order of $K^+ > Na^+ \cong Ca^+ > Mg^{2+}$. The average

water coordination numbers for Ca^{2+} and Mg^{2+} are 7.3 and 6, respectively. Furthermore, Mg^{2+} is found to bind tightly to six water molecules in an octahedral geometry in agreement with the experiment. The dynamic fluctuations in the first shell coordination number indicate that the lifetime of Ca^{2+}−water coordination is about 18 ps, 10 times longer than the relaxation time previously reported for K^+ or Na^+. Even though Mg^{2+} is only slightly smaller than Ca^{2+}, the lifetime of water molecules around Mg^{2+} is on the order of a few hundreds of picoseconds, such that the desolvation kinetics will have a strong influence on the ability of Mg^{2+} to bind other molecules.

References and Notes

(1) *Handbook on Metalloproteins*; Bertini, I., Ed.; CRC Press: Boca Raton, FL, 2001.
(2) Chaturvedi, U. C.; Shrivastava, R. *FEMS Immunol Med Microbiol* **2005**, *43*, 105.
(3) Caminiti, R.; Licheri, G.; Piccaluga, G.; Pinna, G. *Chem. Phys. Lett.* **1977**, *47*, 275.
(4) Hewish, N. A.; Neilson, G. W.; Enderby, J. E. *Nature* **1982**, *297*, 138.
(5) Jalilehvand, F.; Spangberg, D.; Lindqvist-Reis, P.; Hermansson, K.; Persson, I.; Sandstrom, M. *J. Am. Chem. Soc.* **2001**, *123*, 431.
(6) Fulton, J. L.; Heald, S. M.; Badyal, Y. S.; Simonson, J. M. *J. Phys. Chem. A* **2003**, *107*, 4688.
(7) Megyes, T.; Grosz, T.; Radnai, T.; Bako, I.; Palinkas, G. *J. Phys. Chem. A* **2004**, *108*, 7261.
(8) Lyubartsev, A. P.; Laasonen, K.; Laaksonen, A. *J. Chem. Phys.* **2001**, *114*, 3120.
(9) Lightstone, F. C.; Schwegler, E.; Allesch, M.; Gygi, F.; Galli, G. *ChemPhysChem* **2005**, *6*, 1745.
(10) Lightstone, F. C.; Schwegler, E.; Hood, R. Q.; Gygi, F.; Galli, G. *Chem. Phys. Lett.* **2001**, *343*, 549.
(11) Martinez, J. M.; Pappalardo, R. R.; Marcos, E. S. *J. Am. Chem. Soc.* **1999**, *121*, 3175.
(12) Schwenk, C. F.; Loeffler, H. H.; Rode, B. M. *J. Chem. Phys.* **2001**, *115*, 10808.
(13) Rempe, S. B.; Pratt, L. R. *Fluid Phase Equilib.* **2001**, *183*, 121.
(14) Hofer, T. S.; Tran, H. T.; Schwenk, C. F.; Rode, B. M. *J. Comput. Chem.* **2004**, *25*, 211.
(15) Liu, W. B.; Sakane, S.; Wood, R. H.; Doren, D. *J. J. Phys. Chem. A* **2002**, *106*, 1409.
(16) Martin, R. L.; Hay, P. J.; Pratt, L. R. *J. Phys. Chem. A* **1998**, *102*, 3565.
(17) Paulaitis, M. E.; Pratt, L. R. *(Unfolded Proteins) Adv. Protein Chem.* **2002**, *62*, 283.
(18) Asthagiri, D.; Pratt, L. R.; Paulaitis, M. E.; Rempe, S. B. *J. Am. Chem. Soc.* **2004**, *126*, 1285.
(19) Rempe, S. B.; Asthagiri, D.; Pratt, L. R. *Phys. Chem. Chem. Phys.* **2004**, *6*, 1966.
(20) Grossfield, A.; Ren, P. Y.; Ponder, J. W. *J. Am. Chem. Soc.* **2003**, *125*, 15671.
(21) Dang, L. X. *J. Phys. Chem. B* **2002**, *106*, 10388.
(22) Yague, J. I.; Mohammed, A. M.; Loeffler, H. H.; Rode, B. M. *J. Mol. Struct.-THEOCHEM* **2003**, *620*, 15.
(23) Spangberg, D.; Hermansson, K. *J. Chem. Phys.* **2004**, *120*, 4829.
(24) Grossfield, A. *J. Chem. Phys.* **2005**, *122*.
(25) Ren, P. Y.; Ponder, J. W. *J. Comput. Chem.* **2002**, *23*, 1497.
(26) Ren, P.; Ponder, JW. *J. Phys. Chem. B* **2003**, *107* 5933.
(27) Masia, M.; Probst, M.; Rey, R. *J. Chem. Phys.* **2004**, *121*, 7362.
(28) Thole, B. T. *Chem. Phys.* **1981**, *59*, 341.
(29) Masia, M.; Probst, M.; Rey, R. *J. Chem. Phys.* **2005**, *123*.
(30) Halgren, T. A. *J. Am. Chem. Soc.* **1992**, *114*, 7827.
(31) Frisch, M. J.; Trucks, G. W.; Schlegel, H. B.; Scuseria, G. E.; Robb, M. A.; Cheeseman, J. R.; Montgomery, J. A., Jr.; Vreven, T.; Kudin, K. N.; Burant, J. C.; Millam, J. M.; Iyengar, S. S.; Tomasi, J.; Barone, V.; Mennucci, B.; Cossi, M.; Scalmani, G.; Rega, N.; Petersson, G. A.; Nakatsuji, H.; Hada, M.; Ehara, M.; Toyota, K.; Fukuda, R.; Hasegawa, J.; Ishida, M.; Nakajima, T.; Honda, Y.; Kitao, O.; Nakai, H.; Klene, M.; Li, X.; Knox, J. E.; Hratchian, H. P.; Cross, J. B.; Bakken, V.; Adamo, C.; Jaramillo, J.; Gomperts, R.; Stratmann, R. E.; Yazyev, O.; Austin, A. J.;

Cammi, R.; Pomelli, C.; Ochterski, J. W.; Ayala, P. Y.; Morokuma, K.; Voth, G. A.; Salvador, P.; Dannenberg, J. J.; Zakrzewski, V. G.; Dapprich, S.; Daniels, A. D.; Strain, M. C.; Farkas, O.; Malick, D. K.; Rabuck, A. D.; Raghavachari, K.; Foresman, J. B.; Ortiz, J. V.; Cui, Q.; Baboul, A. G.; Clifford, S.; Cioslowski, J.; Stefanov, B. B.; Liu, G.; Liashenko, A.; Piskorz, P.; Komaromi, I.; Martin, R. L.; Fox, D. J.; Keith, T.; Al-Laham, M. A.; Peng, C. Y.; Nanayakkara, A.; Challacombe, M.; Gill, P. M. W.; Johnson, B.; Chen, W.; Wong, M. W.; Gonzalez, C.; Pople, J. A. *Gaussian 03*, revision C.02; Gaussian, Inc.: Wallingford, CT, 2004.

(32) Ponder, J. W. TINKER: Software Tools for Molecular Design, Version 3.9; Saint Louis, MO, 2001.

(33) Sagui, C.; Pedersen, L. G.; Darden, T. A. *J. Chem. Phys.* **2004**, *120*, 73.

(34) Berendsen, H. J. C.; Postma, J. P. M.; van Gunsteren, W. F.; DiNola, A.; Haak, J. R. *J. Chem. Phys.* **1984**, *81*, 3684.

(35) Jorgensen, W. L.; Ravimohan, C. *J. Chem. Phys.* **1985**, *83*, 3050.

(36) Bennett, C. H. *J. Comput. Phys.* **1976**, *22*, 245.

(37) Shirts, M. R.; Pande, V. S. *J. Chem. Phys.* **2005**, *122*.

(38) Schmid, R.; Miah, A. M.; Sapunov, V. N. *Phys. Chem. Chem. Phys.* **2000**, *2*, 97.

(39) Garde, S.; Hummer, G.; Paulaitis, M. E. *J. Chem. Phys.* **1998**, *108*, 1552.

(40) Rajamani, S.; Ghosh, T.; Garde, S. *J. Chem. Phys.* **2004**, *120*, 4457.

(41) Mills, R.; Lobo, V. M. M. *Self-Diffusion in Electrolyte Solutions*; Elsevier: Amsterdam, 1989.

(42) Koneshan, S.; Rasaiah, J. C.; Lynden-Bell, R. M.; Lee, S. H. *J. Phys. Chem. B* **1998**, *102*, 4193.

(43) Guardia, E.; Sese, G.; Padro, J. A.; Kalko, S. G. *J. Solution Chem.* **1999**, *28*, 1113.